

# Radiation and Temperature Effects in Gallium Arsenide, Indium Phosphide, and Silicon Solar Cells

(NASA-TM-89870) RADIATION AND TEMPERATURE  
EFFECTS IN GALLIUM ARSENIIDE, INDIUM  
PHOSPHIDE AND SILICON SOLAR CELLS (NASA)  
14 p Avail: NTIS HC A02/MF A01 CSCL 09C

N87-22098

H1/33 H1/33  
Unclas 0072143

I. Weinberg, C.K. Swartz, and R.E. Hart, Jr.  
*Lewis Research Center*  
*Cleveland, Ohio*

and

R.L. Statler  
*Naval Research Laboratory*  
*Washington, D.C.*

Prepared for the  
19th Photovoltaic Specialists Conference  
sponsored by the Institute of Electrical and Electronics Engineers  
New Orleans, Louisiana, May 4-8, 1987



ORIGINAL PAGE IS  
OF POOR QUALITY

RADIATION AND TEMPERATURE EFFECTS IN GALLIUM ARSENIDE, INDIUM PHOSPHIDE, AND SILICON SOLAR CELLS

I. Weinberg, C.K. Swartz, and R.E. Hart, Jr.  
National Aeronautics and Space Administration  
Lewis Research Center  
Cleveland, Ohio 44135

and

R.L. Statler  
Naval Research Laboratory  
Washington, D.C.

E-3546

The effects of radiation on performance are determined for both n<sup>+</sup>p and p<sup>+</sup>n GaAs and InP cells and for silicon n<sup>+</sup>p cells. It is found that the radiation resistance of InP is greater than that of both GaAs and Si under 1 MeV electron irradiation. For silicon, the observed decreased radiation resistance with decreased resistivity is attributed to the presence of a radiation induced boron-oxygen defect. Comparison of radiation damage in both p<sup>+</sup>n and n<sup>+</sup>p GaAs cells yields a decreased radiation resistance for the n<sup>+</sup>p cell attributable to increased series resistance, decreased shunt resistance, and relatively greater losses in the cell's p-region. For InP, the n<sup>+</sup>p configuration is found to have greater radiation resistance than the p<sup>+</sup>n cell. The increased loss in this latter cell is attributed to losses in the cell's emitter region. Temperature dependency results are interpreted using a theoretical relation for  $dV_{oc}/dT$  which predicts that increased  $V_{oc}$  should result in decreased numerical values for  $dP_m/dT$ . The predicted correlation is observed for GaAs but not for InP a result which is attributed to variations in cell processing.

Introduction

Photovoltaic arrays based on silicon are, at present, the major primary source of spacecraft electric power. On the other hand, gallium arsenide solar cells are beginning to see limited use in applications where end-of-life array output power, in a degrading radiation environment, is a major design consideration. Compared to these latter two cells, indium phosphide solar cells are in a relatively early stage of development. However, it has been shown that InP solar cells are significantly more radiation resistant than either GaAs or silicon when exposed to 1 MeV electron and 10 MeV proton irradiations.<sup>1,2</sup> Their superior radiation resistance, annealability,<sup>3</sup> and the recent attainment of 17.9 percent total area AMO efficiencies,<sup>4</sup> with feasibility indicated for efficiencies greater than 20 percent,<sup>5</sup> make InP cells prime candidates for future use in the space radiation environment. This being the case, it is conceivable that all three cell types will eventually be used in space, their utilization depending on the spacecraft EOL power requirements in a

specific radiation environment. At present, the n<sup>+</sup>p configuration is preferred exclusively for silicon cells used in space. This follows from a demonstrated superior radiation resistance when compared to the p<sup>+</sup>n configuration.<sup>6</sup> However, the situation is unclear with respect to cells based on InP and GaAs. For GaAs, a preliminary comparison of the two configurations has been conducted after proton irradiation.<sup>7</sup> Considering InP, there is a scarcity of data in the open literature comparing the radiation resistance of the two configurations. Hence, we have irradiated InP and GaAs solar cells with 1 MeV electrons in both the n<sup>+</sup>p and p<sup>+</sup>n configurations and determined their performance as a function of fluence. In addition, we have determined temperature dependencies of the solar cell parameters for the unirradiated cells. Our objective lies in assessing the relative performance of n<sup>+</sup>p and p<sup>+</sup>n InP and GaAs cells and thus contributing to a relatively scarce data base. We also summarize the state-of-the-art in AMO efficiency achievements for Si, GaAs, and InP and include comparative radiation resistance data for all three cell types.

Experimental

Details of the InP and GaAs solar cells used in the present radiation damage experiments are shown in Figs. 1 and 2 and Tables I and II. The GaAs cells were obtained from Varian.<sup>8</sup> The n<sup>+</sup>p cells were processed by the Rensselaer Polytechnic Institute,<sup>9</sup> while the p<sup>+</sup>n cells were obtained from Arizona State University. Additional cell details can be found in the figures and in Refs. 8 to 10. The cells were irradiated by 1 MeV electrons in the Naval Research Laboratories Van de Graaf accelerator. Solar cell performance measurements were carried out at NASA Lewis, using an air mass zero X-25 Xenon arc solar. The cell performance data is based on total cell area including that covered by the front contacts. Temperature dependency measurements on unirradiated cells were performed in a nitrogen atmosphere using a variable temperature chamber into which the X-25 simulator beam was introduced through a glass port. In a later section of the present paper we compare the performance of Si, GaAs, and InP cells under 1 MeV electron irradiation. For background information to this comparison we present in Table III, the performance parameters of those cells having the

highest AMO efficiencies. Additional details can be found in Refs. 4, 8, 11, and 12.

### Results

Normalized efficiencies of the GaAs and InP cells are shown in Figs. 3 and 4. From the figures it is seen that the radiation resistance of the InP cells is greater than GaAs cells under 1 MeV electron irradiation.<sup>1,2</sup> From Fig. 3 it is seen that the radiation resistance of the GaAs p-n cells are significantly greater than that of the n-p cells under the present irradiations. For InP, the n-p cells exhibit higher radiation resistance (Fig. 4). The behavior of the remaining cell parameters at constant high fluence is summarized in Tables III and IV.

Previous results have shown that, when plotted on a normalized basis, the radiation resistance of InP cells is greater than that of either GaAs or Si.<sup>2,13</sup> The present data is found to be in agreement with this result (Fig. 5). In the figure, data for the cell labeled InP (dark) and the GaAs cells are obtained from the present results. The cell labeled InP (dark) was irradiated by 1 MeV electrons in the absence of light. It has been found that irradiation of InP cells with the cell illuminated by light results in increased radiation resistance due to photoinjection of minority carriers.<sup>14</sup> Thus, the cell labeled InP (illuminated) was irradiated under a light intensity of 70 mW/cm<sup>2</sup>. Data for this latter cell was obtained from Ref. 14, while that for the 10  $\Omega$ -cm Si cell was obtained from the JPL radiation handbook.<sup>15</sup> The low resistivity silicon cells (0.1 and 0.2  $\Omega$ -cm) are similar in design to the high efficiency silicon cells in Table III. Typical temperature dependency runs for GaAs and InP over a wide range of temperature are shown in Figs. 6 and 7. In general, over most of the temperature range, maximum power ( $P_{max}$ ),  $V_{oc}$ , and fill factor (FF) decrease with increasing temperature while  $I_{sc}$  increases with temperature.

### Discussion

#### Radiation Effects in Silicon

The decreased radiation resistance with decreasing cell base resistivity, observed in Fig. 5, is typical of the behavior observed for silicon solar cells. This follows, empirically, from the behavior of the diffusion length damage coefficient  $K_L$ .<sup>17,18</sup> It has been found for cells with base resistivity  $\rho_B$  between 0.1 and 20  $\Omega$ -cm that  $K_L$  is proportional to  $(1/\rho_B^{2/3})$ .<sup>17,18</sup> Since decreasing values of  $K_L$  imply a smaller radiation induced reduction of minority carrier diffusion length,<sup>15</sup> the resistivity dependence of  $K_L$  implies that for silicon, in this resistivity range, radiation resistance increases as cell base resistivity increases. The data of Fig. 5 supports this conclusion.

A more fundamental reason for the resistivity dependent performance of irradiated silicon can be found in the behavior of defects observed by Deep

Level Transient Spectroscopy (DLTS). Evidence obtained from DLTS has led to the conclusion that a radiation induced defect, composed of boron and oxygen, is predominant in causing radiation induced degradation in boron doped p-type silicon.<sup>19,20</sup> Of the three major deep level defects observed in electron irradiated silicon, only the boron-oxygen defect exhibits an increasing concentration with decreasing cell resistivity.<sup>21</sup> Hence, the decreased radiation resistance, with decreasing cell base resistivity, noted from Fig. 5, is attributed to the consequent increasing concentration of this defect. This fundamental limitation presents a barrier to the use of low resistivity boron-doped, silicon solar cells in the space radiation environment.

#### Radiation Effects in GaAs and InP

The superior radiation resistance of n-p silicon cells over the p-n configuration has long been an established fact. However, the preference of one configuration over the other is far from established for either InP or GaAs.

For gallium arsenide, the thinner emitter region of the present n-p cell could lead to the prediction of increased radiation resistance for this cell. This would seem to follow from previous results on LPE grown GaAs cells where it was observed that radiation resistance tended to increase with decreasing emitter thickness.<sup>22</sup> However, despite the decreased emitter thickness the present n-p GaAs cell exhibits significantly decreased radiation resistance. To examine this behavior in greater detail, we consider the I-V curves of the irradiated and unirradiated GaAs cells (Figs. 8 and 9). From Fig. 9, relatively small changes are indicated, for the p-n cell, in both series and shunt resistance after irradiation. However, for the n-p cell, Fig. 8 indicates a relatively large decrease in shunt resistance and a relatively large increase in series resistance. These effects result in decreased solar cell output and thus decreased efficiency. The relatively large decrease in  $I_{sc}$  noted for the n-p cell (Table IV) is another factor resulting in decreased efficiency. This loss occurs predominantly in the cell's base or p-region (Fig. 10) and is primarily due to a decrease in diffusion length due to radiation. Thus, the decreased radiation resistance of the GaAs n-p cell is attributed to the radiation induced increased series resistance, decreased shunt resistance, and decreased short circuit current due to defect generation in the cell's p-region.

Considering InP, from Table V, the change in fill factor, after irradiation, is relatively small and approximately the same for both configurations. Hence relative changes in shunt and series resistances are not significant factors in comparing the radiation resistance of the two configurations. Similarly, the percentage change in  $V_{oc}$  is approximately the same for both cell types. On the other hand, the percentage loss in  $I_{sc}$  is slightly, but definitely larger for the p-n cell. For further consideration of the loss in  $I_{sc}$  we

consider the normalized spectral response versus wavelength shown in Figs. 11 and 12. In the figures,  $(I_{sc}(\lambda))_{\phi}$  is short circuit current at wavelength  $\lambda$  and 1 MeV electron fluence  $\phi$ , while  $(I_{sc}(\lambda))_0$  is short circuit current in the unirradiated cell at the same wavelength. The position of the p-n junction is computed from the optical path length  $1/\alpha(\lambda)$  where  $\alpha(\lambda)$  is the absorption coefficient of InP at wavelength  $\lambda$ .<sup>23</sup> From the figures it is seen that most of the current loss occurs in the emitter region of the p-n cell and in the base of the n-p cell. From previous results, it has been demonstrated that, for n-p InP cells, radiation resistance increases as p-dopant concentration (zinc) increases.<sup>13</sup> Since the zinc p-dopant concentration in the p-n cell is at least an order of magnitude greater than the zinc p-dopant concentration in the present n-p InP cell and since most of the damage occurs in the p-regions of both cells one would a priori expect comparatively less radiation resistance in the present n-p cell. Since this is not the case for the present cells, the current results are considered to be anomalous. In any event, it is concluded that the relatively decreased radiation resistance of the p-n cell is due to comparatively greater losses in the heavily doped emitter region.

#### Temperature Dependency

To consider the temperature dependency of unirradiated InP and GaAs over the wide range of temperatures shown in Figs. 6 and 7 would be a highly complex undertaking for any large group of cells. The present discussion is simplified by considering the temperature dependencies of the solar cell parameters at a single temperature. Since solar cells in low earth and geosynchronous orbits operate at temperatures near 60 °C, we chose this temperature for the present considerations.

Data for the temperature variation of  $P_{max}$ ,  $V_{oc}$ ,  $I_{sc}$ , and  $FF$  at 60 °C are shown in Tables VI and VII. The temperature dependencies of  $P_{max}$ , the cell maximum power, are summarized graphically in Fig. 13. The wide spread in values, obtained for this parameter, emphasizes the importance of independently determining temperature dependencies for any group of cells intended for a specific mission.

To consider the relative importance of the various cell parameters in determining the temperature dependency of  $P_{max}$ , the temperature dependencies are expressed in relative terms using the relation<sup>24</sup>

$$\frac{1}{P_{max}} \frac{dP_{max}}{dT} = \frac{1}{I_{sc}} \frac{dI_{sc}}{dT} + \frac{1}{V_{oc}} \frac{dV_{oc}}{dT} + \frac{1}{FF} \frac{dFF}{dT} \quad (1)$$

Average values, for the cells of Tables VI and VII, for each term in the preceding relation, are shown in Figs. 14 and 15. Considering terms on the right hand side of Eq. (1), the figures indicate that the term in  $V_{oc}$  is clearly the largest in magnitude for both cell types. Hence,  $dP_{max}/dT$  is assumed to be most dependent on the temperature variation

of  $V_{oc}$ . To consider this latter temperature variation in greater detail, we use the relation<sup>24</sup>

$$\frac{dV_{oc}}{dT} = \frac{V_{oc} - E_g(T)}{T} - \frac{3k}{q} - \frac{\alpha T(T + 2\beta)}{(T + \beta)^2} + \frac{kT}{qI_{sc}} \frac{dI_{sc}}{dT} \quad (2)$$

where  $E_g(T)$  is the bandgap at temperature  $T$ ,  $q$  is the electronic charge,  $k$  is the Boltzmann constant, and  $\alpha$  and  $\beta$  are constants in the temperature dependency of  $E_g(T)$  with

$$E_g(T) = E_g(0) - \frac{\alpha T^2}{(T + \beta)} \quad (3)$$

where  $E_g(0)$  is the bandgap at 0 K. The parameters required in evaluating  $E_g(T)$  are given in Table VIII.

The results of calculations using Eqs. (2) and (3) are shown in Table IX where reasonable agreement is found between the experimental and calculated values for both InP and GaAs. Considering the success of Eq. (2) in predicting the values of  $dV_{oc}/dT$ , and noting that the term in  $I_{sc}$  is negligible, it follows that if  $dP_{max}/dT$  is proportional to  $dV_{oc}/dT$ , then increased values of  $V_{oc}$  should result in lower numerical values of  $dP_{max}/dT$ . From Fig. 16, it is seen that  $dP_{max}/dT$  is roughly proportional to  $dV_{oc}/dT$  for GaAs, while for InP no such correlation exists (Fig. 17). From the preceding, it follows that a correlation should exist between  $V_{oc}$  and  $dP_{max}/dT$  for GaAs, while no such correlation should exist for InP. That this is the case can be seen from the data of Fig. 18. Thus, the spread in values in  $dP_{max}/dT$ , exhibited by GaAs in Fig. 13 is attributed to variations in open circuit voltage.

It is noted that, in Fig. 18, the GaAs cells are grouped around two values of  $V_{oc}$ . The five cells grouped around the highest  $V_{oc}$  are AlGaAs/GaAs heteroface cells while the remaining cells grouped around the lower  $V_{oc}$  are simple GaAs homojunctions. Average values for these cell groups are shown, together with an average value for the InP cells, in Table X. Following the prediction based on Eq. (2), it is noted that the GaAs cells with the highest  $V_{oc}$  have the lowest numerical value of  $dP_{max}/dT$ . The absence of even such a gross correlation for the present InP cells indicates that temperature dependent factors, other than  $dV_{oc}/dT$  are significant in determining the temperature dependency of  $P_{max}$  for these cells. This could arise from variations in the temperature dependencies of factors such as series and shunt resistance which in turn could result from variations in cell processing.

#### Conclusion

It has been shown, in agreement with previous results, that the radiation resistance of InP solar cells is superior to both GaAs and Si under 1 MeV electron irradiation. The present n-p indium

phosphide cells are found to be slightly more radiation resistance than p-n cells under 1 MeV electron irradiations. This is attributed to degradation in the latter cell's heavily doped p-type emitter region. For GaAs, the p-n configuration is significantly more radiation resistant than the n-p cells. The increased degradation in this latter cell can be attributed to radiation induced increases in series resistance, decreased shunt resistance and degradation in the p-base

Temperature dependency experiments yield a theoretically predicted correlation between  $dP_{max}/dT$  and  $V_{oc}$  for GaAs, but none for InP. The spread in  $dP_{max}/dT$  values observed for the present GaAs cells is thus attributed to variations in open circuit voltage. The GaAs cells can be divided into two groups clustering around high  $V_{oc}$  and low  $V_{oc}$  corresponding to low and high numerical values respectively for  $dP_{max}/dT$ . The high  $V_{oc}$  group yields an average  $dP_{max}/dT$  value of  $-(4.35 \pm 0.35) \times 10^{-2} \text{ mW/cm}^2 \text{ K}$  while the low voltage GaAs group has the average value  $-(6.04 \pm 0.01) \times 10^{-2} \text{ mW/cm}^2 \text{ K}$ . For InP, the average value for 6 cells is  $-(5.3 \pm 1.2) \times 10^{-2} \text{ mW/cm}^2 \text{ K}$ . The spread in values observed for these cells indicates that great care should be exercised in applying published temperature dependency calculations to numerical predictions of solar cell performance in a given space environment.

#### References

1. A. Yamamoto, M. Yamaguchi, and C. Uemura, "High Conversion Efficiency and High Radiation Resistance InP Homo Junction Solar Cells," Appl. Phys. Lett., vol. 44, pp. 611-613, 1984.
2. I. Weinberg, C.K. Swartz, and R.E. Hart, Jr., "Potential for Use of InP Solar Cells in the Space Radiation Environment," in 18th IEEE Photovoltaic Specialists Conference, IEEE, 1985, pp. 1722-1724.
3. M. Yamaguchi, K. Ando, A. Yamamoto, and C. Uemura, "Minority Carrier Injection Annealing of Electron Irradiation-Induced Defects in InP Solar Cells," Appl. Phys. Lett., vol. 44, pp. 432-434, 1984.
4. M.B. Spitzer, C.V. Keavney, and S.M. Vernon, "Junction Formation Techniques for Indium Phosphide Solar Cells," to be presented at the 19th Photovoltaic Specialists Conference, New Orleans, LA, May 4-9, 1987.
5. C. Goradia, J.V. Gier, and I. Weinberg, "Modelling and Design of High Efficiency Radiation Tolerant InP Space Solar Cells," to be presented at the 19th IEEE Photovoltaic Specialists Conference, New Orleans, LA, May 4-9, 1987.
6. J. Mandelkorn, C. McAfee, J. Kesperis, L. Schwartz, and W. Pharo, "Fabrication and Characteristics of Phosphorus-Diffused Silicon Solar Cells," J. Electrochem. Soc., vol. 109, pp. 313-318, 1962.
7. I. Weinberg, C.K. Swartz, and R.E. Hart, Jr., "Performance and Temperature Dependencies of Proton Irradiated n/P and P/n GaAs n/P Silicon Cells," in 18th IEEE Photovoltaic Specialists Conference, IEEE, 1985, pp. 344-349.
8. J.G. Werthen, G.F. Virshup, C.W. Ford, C.R. Lewis, and H.C. Hamaker, "21% (one sun, air mass zero)  $4 \text{ cm}^2$  GaAs Space Solar Cells," Appl. Phys. Lett., vol. 48, pp. 74-75, 1986.
9. K.K. Parat, S. Bothra, J.M. Borrego, and S.K. Ghandhi, "Solar Cells in Bulk InP, Made by an Open Tube Diffusion Process," Solid State Electron., vol. 30, pp. 283-287, 1987.
10. K.Y. Choi and C.C. Shen, "P/N InP Homo Junction Solar Cells by LPE and MOCVD Techniques," to be presented at 19th IEEE Photovoltaic Specialists Conference, New Orleans, LA, May 4-9, 1987.
11. M.A. Green, A.W. Blakers, S.R. Wenham, S. Narayanan, M.R. Willison, M. Taouk, and S. Szpitalak, "Improvements in Silicon Solar Cell Efficiency," in 18th IEEE Photovoltaic Specialists Conference, IEEE, 1987, pp. 39-42.
12. G. Grotty, R. Kachare, and B.E. Anspaugh, "A New High-Efficiency Silicon Solar Cell for Potential Space Applications," to be presented at 19th IEEE Photovoltaic Specialists Conference, New Orleans, LA, May 4-9, 1987.
13. M. Yamaguchi, C. Uemura, A. Yamamoto, and A. Shibukawa, "Electron Irradiation Damage in Radiation-Resistant InP Solar Cells," Jpn. J. Appl. Phys., vol. 23, pp. 302-307, 1984.
14. K. Ando and M. Yamaguchi, "Radiation Resistance of InP Solar Cells Under Light Illumination," Appl. Phys. Lett., vol. 47, pp. 846-848, 1985.
15. H.Y. Tada, B.R. Anspaugh, and R.G. Downing, Solar Cell Radiation Handbook, 3rd ed., JPL-PUB-82-69, Jet Propulsion Laboratory, California Institute of Technology, Pasadena, CA, 1982. (Also, NASA CR-169662).
16. V.G. Welzer, I. Weinberg, and C.K. Swartz, "Radiation Tolerance of Low Resistivity, High Voltage Silicon Solar Cells," in Space Photovoltaic Research and Technology 1983, NASA CP-2314, 1983, pp. 74-80.

17. J.R. Srouer, S. Othmer, K.Y. Chiu, and O.L. Curtis, Jr., "Damage Coefficients in Low Resistivity Silicon," NASA CR-134768, 1975.
18. J.R. Srouer, S. Othmer, K.Y. Chiu, and O.L. Curtis, Jr., "Electron and Proton Damage Coefficients in Low-Resistivity Bulk Silicon and Silicon Solar Cells," in High Efficiency Silicon Solar Cell Review, NASA TM-X-3326, 1975, pp. 51-59.
19. I. Weinberg, S. Mehta, and C.K. Swartz, "Increased Radiation Resistance in Lithium-Counterdoped Silicon Solar Cells," Appl. Phys. Lett., vol. 44, pp. 1071-1073, 1987.
20. I. Weinberg, C. Goradia, J.W. Stupica, and C.K. Swartz, "Cell Performance and Defect Behavior in Proton-Irradiated Lithium-Counterdoped n-p Silicon Solar Cells," J. Appl. Phys., vol. 60, pp. 2179-2181, 1986.
21. P.M. Mooney, L.J. Cheng, M. Suli, J.D. Gerson, and J.W. Corbett, "Defect Energy Levels in Boron-Doped Silicon Irradiated with 1-MeV Electrons," Phys. Rev. B, vol. 15, pp. 3836-3843, 1977.
22. R. Loo, G.S. Kamath, and R.C. Knechtli, "Radiation Damage in GaAs Solar Cells," in 14th IEEE Photovoltaic Specialists Conference, IEEE, 1980, pp. 1090-1097.
23. O.J. Glembocki, H. Pillar, "Indium Phosphide (InP)," in Handbook of Optical Constants of Solids, E. D. Palik, Ed., New York: Academic Press, 1985, pp. 503-516.
24. J.C.C. Fan, "Theoretical Temperature Dependency of Solar Cell Parameters," Solar Cells, 17, pp. 309-315, 1986.

TABLE I. - GaAs PREIRRADIATION PERFORMANCE PARAMETERS

Cell	Efficiency, percent	Voc, V	JSC, ma/cm <sup>2</sup>	FF, percent
n <sup>+</sup> p	18.8	1.018	30.6	82.8
	19.8	1.034	30.9	85
p <sup>+</sup> n	19.6	1.041	31.8	81.2
	19.8	1.044	32.1	81.1

TABLE II. - InP PREIRRADIATION PERFORMANCE PARAMETERS

Cell	Efficiency, percent	Voc, V	JSC, ma/cm <sup>2</sup>	FF, percent
n <sup>+</sup> p	12.9	0.815	26.3	82.6
	12.7	.814	26	82.3
p <sup>+</sup> n	13.9	0.843	32.4	70
	14.7	.858	33	71

TABLE III. - STATE-OF-THE-ART SOLAR CELLS

Cell	Efficiency, <sup>a</sup> percent	JSC, ma/cm <sup>2</sup>	Voc, V	FF, percent
InP <sup>b</sup>	17.9	33.9	868	83.8
GaAs <sup>c</sup>	21.1	32.3	1050	84
Si <sup>d</sup>	18.1	44.5	672	82.1
Si <sup>e</sup>	17.7	44.6	660	81.5

<sup>a</sup>All measurements are at air mass zero and include total cell areas.

<sup>b</sup>Ref. 4.

<sup>c</sup>Ref. 9.

<sup>d</sup>Ref. 12.

<sup>e</sup>Ref. 13.

TABLE IV. - NORMALIZED CELL PARAMETERS AT CONSTANT FLUENCE

[GaAs:  $n^+p$  and  $p^+n$ .  $\phi = 1$  MeV electron fluence  
 $= 3 \times 10^{15}/\text{cm}^2$ .]

Cell		$n\phi/\eta_0$	$(I_{sc})_\phi/(I_{sc})_0$	$(V_{oc})_\phi/(V_{oc})_0$	$(FF)_\phi/(FF)_0$
GaAs	$p^+n$	0.68	0.9	0.84	0.93
	$n^+p$	.52	.72	.81	.85

TABLE V. - NORMALIZED CELL PARAMETERS AT CONSTANT HIGH FLUENCE

[InP:  $n^+p$  and  $p^+n$ .  $\phi = 1$  MeV electron fluence  
 $= 3 \times 10^{15}/\text{cm}^2$ .]

Cell		$n\phi/\eta_0$	$(I_{sc})_\phi/(I_{sc})_0$	$(V_{oc})_\phi/(V_{oc})_0$	$(FF)_\phi/(FF)_0$
InP	$p^+n$	0.85	0.96	0.93	0.94
	$n^+p$	.82	.93	.92	.95

TABLE VI. - TEMPERATURE VARIATION TERMS - GaAs

[T = 60 °C.]

Cell	$dP_m/dT$ $\text{mW}/\text{cm}^2 \text{ K}$	$dV_{oc}/dT$ $\text{mV}/\text{K}$	$dI_{sc}/dT$ $\text{mA}/\text{cm}^2 \text{ K}$	$dFF/dT$ $\text{percent}/\text{K}$
GaAs $p/n$	$-4.4 \times 10^{-2}$	-2	$+1.95 \times 10^{-2}$	$-5.4 \times 10^{-2}$
	$-4.92 \times 10^{-2}$	-2.1	$1.97 \times 10^{-2}$	$-6.55 \times 10^{-2}$
	$-4.28 \times 10^{-2}$	-2.05	$2.28 \times 10^{-2}$	$-5.09 \times 10^{-2}$
	$-4. \times 10^{-2}$	-1.97	$1.91 \times 10^{-2}$	$-3.98 \times 10^{-2}$
GaAs $n/p$	$-4.14 \times 10^{-2}$	-1.97	$2.71 \times 10^{-2}$	$-5.44 \times 10^{-2}$
	$-6.04 \times 10^{-2}$	-2.3	$2.03 \times 10^{-2}$	$-8.14 \times 10^{-2}$
	$-6.03 \times 10^{-2}$	-2.3	$2.09 \times 10^{-2}$	$-8.42 \times 10^{-2}$

TABLE VII. - TEMPERATURE VARIATION TERMS - InP

[T = 60 °C; n/p indium phosphide.]

dPm/dT mW/cm <sup>2</sup> K	dVoc/dT mV/K	dIsc/dT mA/cm <sup>2</sup> K	dFF/dT percent/K
-3.13x10 <sup>-2</sup>	-2.31	+3.23x10 <sup>-2</sup>	-2.97x10 <sup>-2</sup>
-4.86x10 <sup>-2</sup>	-2.33	1.69x10 <sup>-2</sup>	-8.6x10 <sup>-2</sup>
-6.23x10 <sup>-2</sup>	-2.32	2.27x10 <sup>-2</sup>	-1.16x10 <sup>-2</sup>
-6.25x10 <sup>-2</sup>	-2.21	1.44x10 <sup>-2</sup>	-9.78x10 <sup>-2</sup>
-5x10 <sup>-2</sup>	-2.38	2.39x10 <sup>-2</sup>	-9.38x10 <sup>-2</sup>
-6.3x10 <sup>-2</sup>	-2.46	1.62x10 <sup>-2</sup>	-1.7x10 <sup>-1</sup>

TABLE VIII. - PARAMETERS USED IN  
CALCULATING BANDGAP TEMPERATURE  
DEPENDENCY

Cell	Eg(0), eV	$\alpha$ eV/K	$\beta$ , K
InP	1.421	6.63x10 <sup>-4</sup>	552
GaAs	1.519	5.405x10 <sup>-4</sup>	204

TABLE IX. - COMPARISON OF CALCULATED AND EXPERIMENTAL  
dVoc/dT VALUES

[T = 60 °C.]

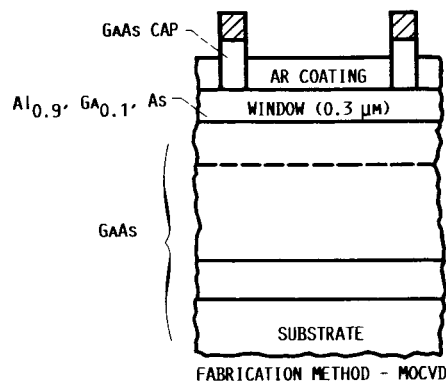
(a) GaAs		(b) InP	
dVoc/dT, mV K <sup>-1</sup>		dVoc/dT, mV K <sup>-1</sup>	
Experimental	Calculated	Experimental	Calculated
-2	-2	-2.31	-2.38
-2.1	-2.1	-2.33	-2.39
-2.05	-2.1	-2.32	-2.32
-1.97	-2.09	-2.21	-2.34
-2.3	-2.36	-2.38	-2.46
-2.3	-2.29	-2.46	-2.45
-1.97	-2.1		

TABLE X. - TEMPERATURE DEPENDENCIES - GaAs and InP

[T = 60 °C.]

Cell		No. of cells	Voc, mV	dVoc/dT, mV/K	dPm/dT mW/cm <sup>2</sup> K
GaAs	AlGaAs/GaAs	5	955±10	-2.02±0.06	-(4.35±0.35)x10 <sup>-2</sup>
	Homojunction	2	886±11	-2.3	-(6.04±.01)x10 <sup>-2</sup>
InP	Homojunction	6	744±15	-2.34±0.08	-(5.3±1.2)x10 <sup>-2</sup>





n+p CELL			
TYPE	THICKNESS, $\mu\text{m}$	DOPANT	
		ATOM	CONCENTRATION, $\text{cm}^{-3}$
n	0.2	SE	$1.5 \times 10^{18}$
p	3	ZN	$7 \times 10^{17}$
p	.5	ZN	$8 \times 10^{18}$

p+n CELL			
TYPE	THICKNESS, $\mu\text{m}$	DOPANT	
		ATOM	CONCENTRATION, $\text{cm}^{-3}$
p	0.5	Mg	$1.5 \times 10^{18}$
n	3	SE	$7 \times 10^{17}$
n	.5	SE	$8 \times 10^{18}$

CO-87-26192

FIGURE 1. - GAAS CELL CONFIGURATIONS.

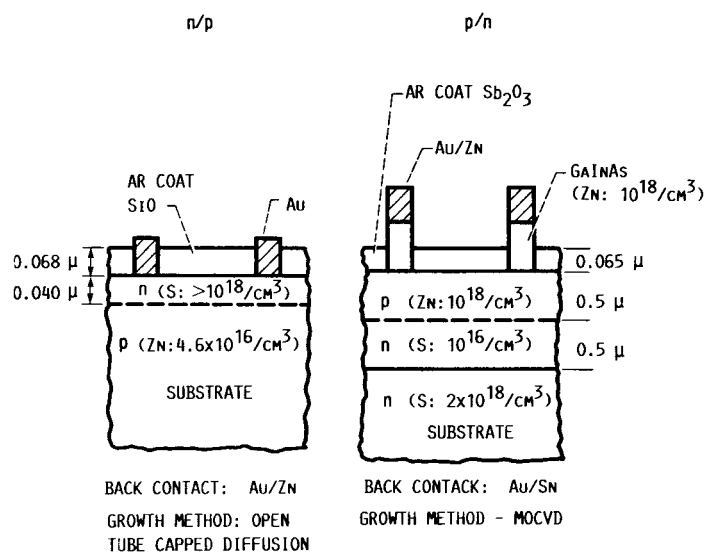


FIGURE 2. - InP CELL CONFIGURATION.

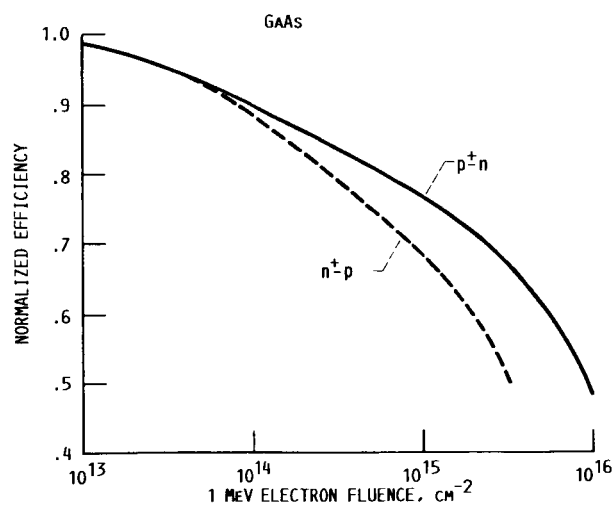


FIGURE 3. - NORMALIZED EFFICIENCY AFTER 1 MeV ELECTRON IRRADIATION - GAAS.

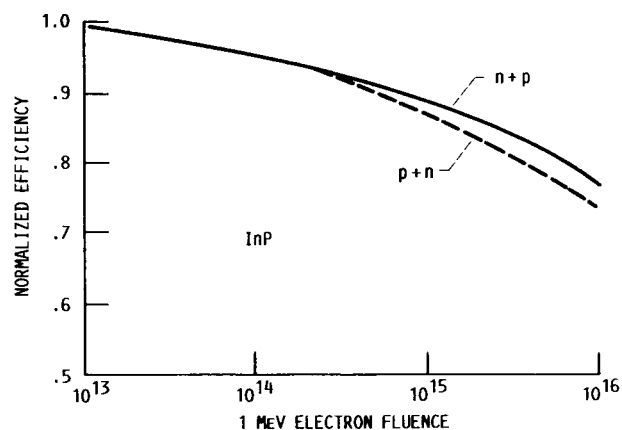


FIGURE 4. - NORMALIZED EFFICIENCY AFTER 1 MeV ELECTRON IRRADIATION - I P.

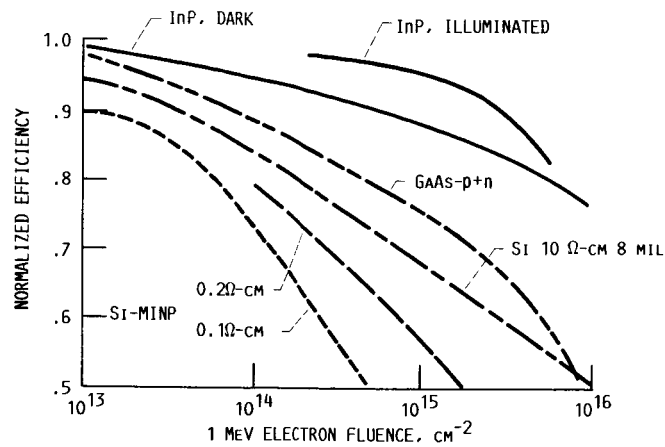


FIGURE 5. - NORMALIZED EFFICIENCIES OF InP, GAAS AND SI AFTER 1 MeV ELECTRON IRRADIATION.

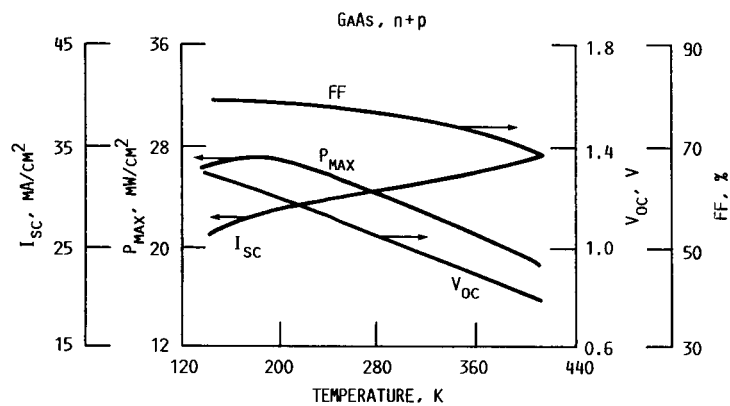


FIGURE 6. - VARIATION OF CELL PARAMETERS WITH TEMPERATURE FOR GAAS.

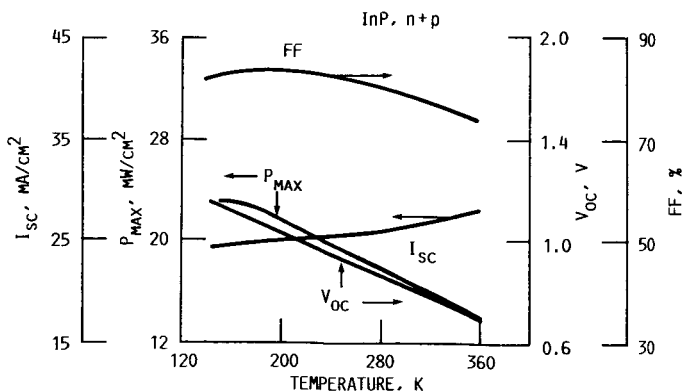


FIGURE 7. - VARIATION OF CELL PARAMETERS WITH TEMPERATURE FOR InP.

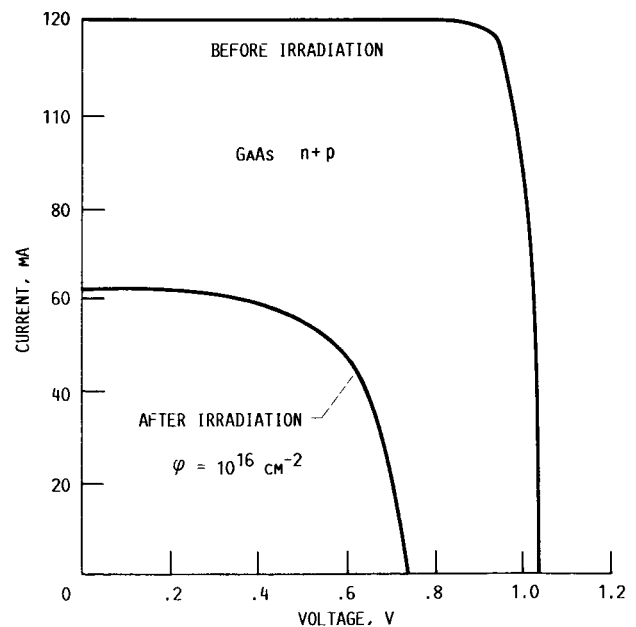


FIGURE 8. - I-V CURVES FOR n+p GAAS CURVES - IRRADIATION BY 1 MeV ELECTRONS.

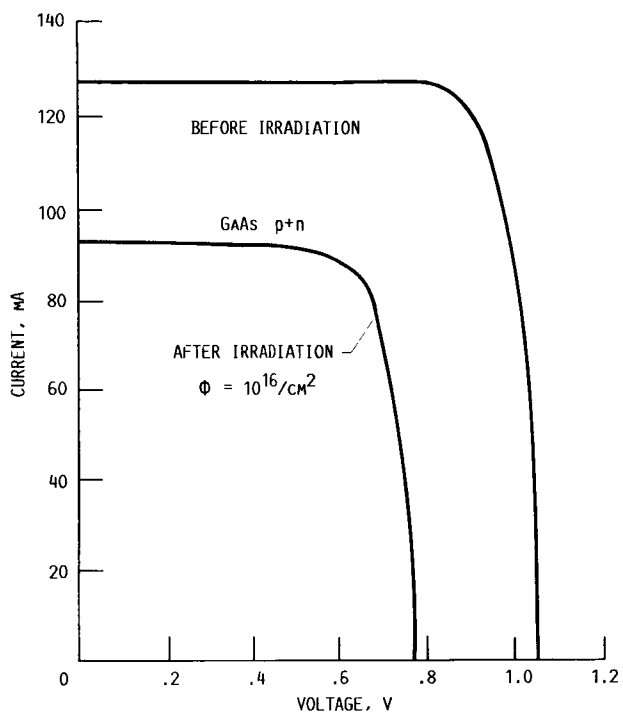


FIGURE 9.- I-V CURVES FOR p+n GAAs-IRRADIATION BY 1 MeV ELECTRONS.

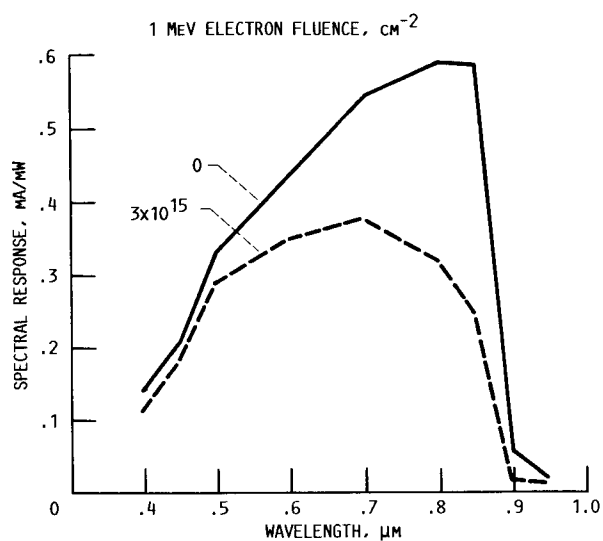


FIGURE 10. - SPECTRAL RESPONSE OF GAAs n+p CELL.

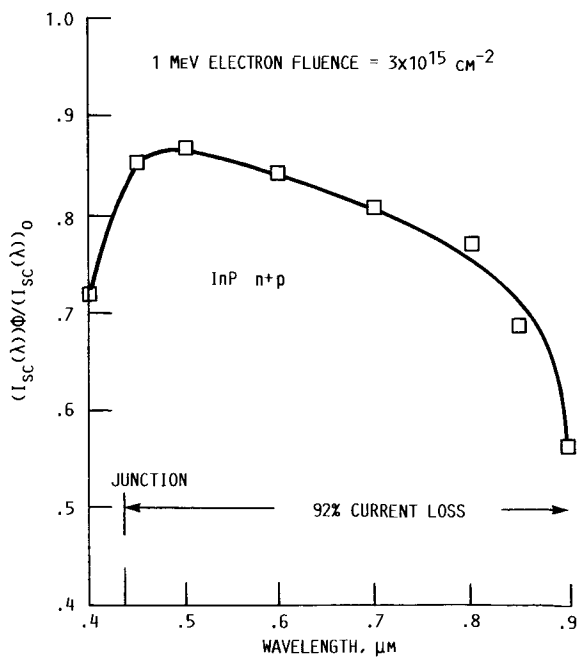


FIGURE 11. - NORMALIZED SPECTRAL RESPONSE OF n+p InP CELL.

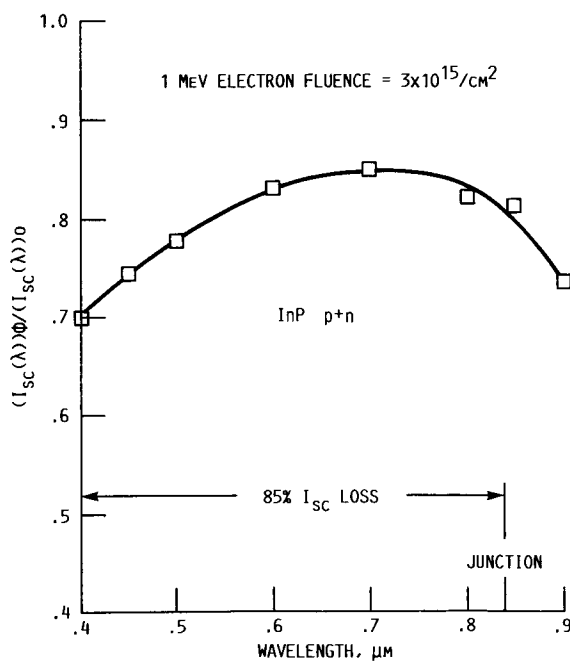


FIGURE 12. - NORMALIZED SPECTRAL RESPONSE OF p+n InP CELL.

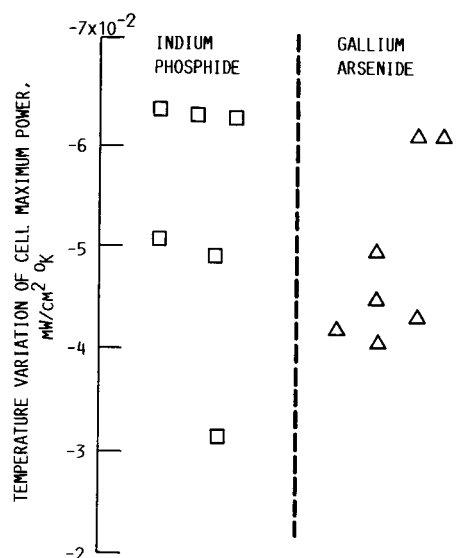


FIGURE 13. - TEMPERATURE VARIATION OF MAXIMUM POWER FOR UNIRRADIATED INDIUM PHOSPHIDE AND GALLIUM ARSENIDE SOLAR CELLS.

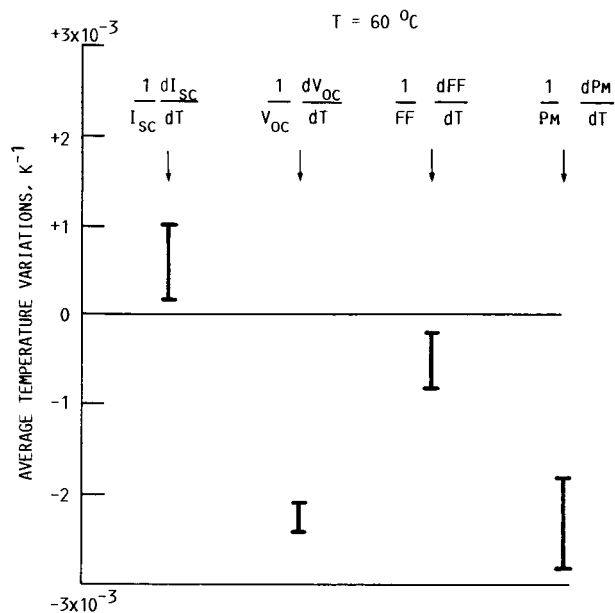


FIGURE 14. - GAAS TEMPERATURE VARIATION TERMS - AVERAGE VALUES.

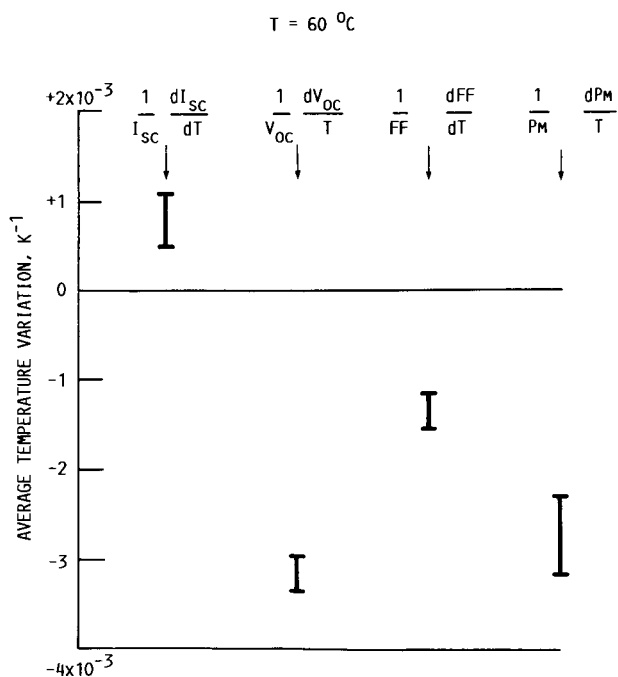


FIGURE 15. - INP TEMPERATURE VARIATION TERMS AVERAGE VALUES.

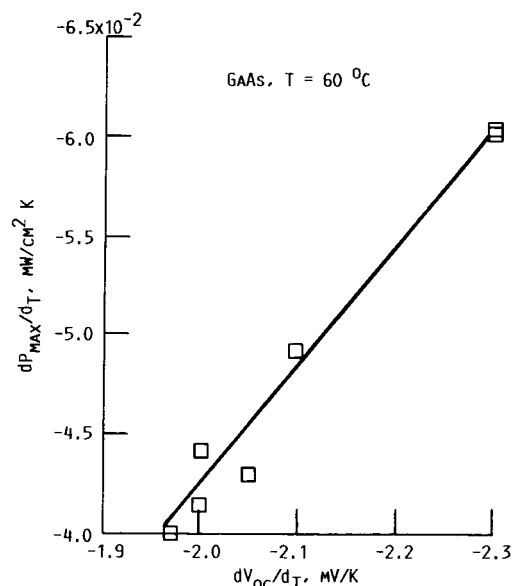


FIGURE 16. - MAXIMUM POWER VARIATION VERSUS  $V_{oc}$  TEMPERATURE VARIATION.

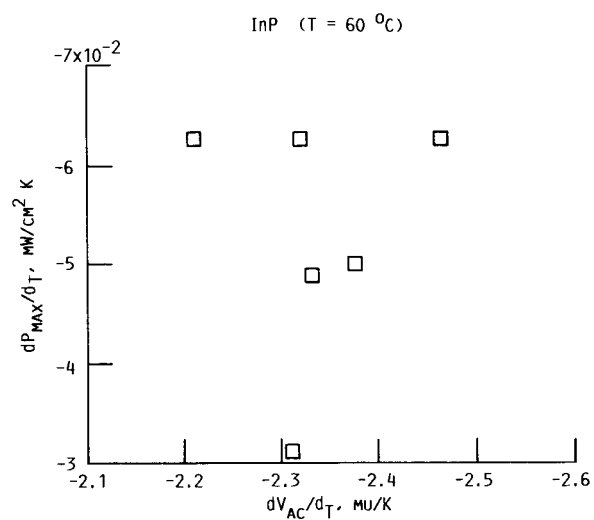


FIGURE 17.-  $P_{MAX}$  TEMPERATURE VARIATION VERSUS  $V_{OC}$  TEMPERATURE VARIATION.

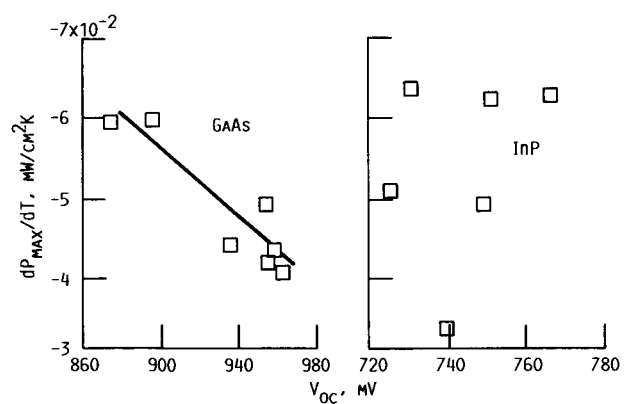


FIGURE 18. -  $P_{MAX}$  TEMPERATURE VARIATION VESUS  $V_{OC}$  TEMPERATURE VARIATION GAAS AND InP.

1. Report No. <b>NASA TM-89870</b>		2. Government Accession No.		3. Recipient's Catalog No.	
4. Title and Subtitle  <b>Radiation and Temperature Effects in Gallium Arsenide, Indium Phosphide, and Silicon Solar Cells</b>				5. Report Date	
				6. Performing Organization Code  <b>506-41-11</b>	
7. Author(s)  <b>I. Weinberg, C.K. Swartz, R.E. Hart, Jr., and R.L. Statler</b>				8. Performing Organization Report No.  <b>E-3546</b>	
				10. Work Unit No.	
9. Performing Organization Name and Address  <b>National Aeronautics and Space Administration Lewis Research Center Cleveland, Ohio 44135</b>				11. Contract or Grant No.	
				13. Type of Report and Period Covered  <b>Technical Memorandum</b>	
12. Sponsoring Agency Name and Address  <b>National Aeronautics and Space Administration Washington, D.C. 20546</b>				14. Sponsoring Agency Code	
15. Supplementary Notes  <b>Prepared for the 19th Photovoltaic Specialists Conference sponsored by the Institute of Electrical and Electronics Engineers, New Orleans, Louisiana, May 4-8, 1987. I. Weinberg, C.K. Swartz, and R.E. Hart, Jr., NASA Lewis Research Center; R.L. Statler, Naval Research Laboratory, Washington, D.C.</b>					
16. Abstract  <b>The effects of radiation on performance are determined for both n<sup>+</sup>p and p<sup>+</sup>n GaAs and InP cells and for silicon n<sup>+</sup>p cells. It is found that the radiation resistance of InP is greater than that of both GaAs and Si under 1 MeV electron irradiation. For silicon, the observed decreased radiation resistance with decreased resistivity is attributed to the presence of a radiation induced boron-oxygen defect. Comparison of radiation damage in both p<sup>+</sup>n and n<sup>+</sup>p GaAs cells yields a decreased radiation resistance for the n<sup>+</sup>p cell attributable to increased series resistance, decreased shunt resistance, and relatively greater losses in the cell's p-region. For InP, the n<sup>+</sup>p configuration is found to have greater radiation resistance than the p<sup>+</sup>n cell. The increased loss in this latter cell is attributed to losses in the cell's emitter region. Temperature dependency results are interpreted using a theoretical relation for dVoc/dT which predicts that increased Voc should result in decreased numerical values for dPm/dT. The predicted correlation is observed for GaAs but not for InP a result which is attributed to variations in cell processing.</b>					
17. Key Words (Suggested by Author(s))  <b>Solar cells; Radiation damage; Silicon; Gallium arsenide indium phosphide</b>				18. Distribution Statement  <b>Unclassified - unlimited STAR Category 33</b>	
19. Security Classif. (of this report)  <b>Unclassified</b>		20. Security Classif. (of this page)  <b>Unclassified</b>		21. No. of pages  <b>14</b>	
				22. Price*  <b>A02</b>	